Peak Trabecular Bone Microstructure Predicts Rate of Estrogen-Deficiency-Induced Bone Loss in Rats

Yihan Li¹ (<u>yihanl@seas.upenn.edu</u>), Wei-Ju Tseng¹ (<u>weits@pennmedicine.upenn.edu</u>), Chantal

M. J. de Bakker^{1,2} (chantal.debakker@ucalgary.ca), Hongbo Zhao¹

(zhhongbo@pennmedicine.upenn.edu), Rebecca Chung¹

(rebecca.chung@pennmedicine.upenn.edu), and X. Sherry Liu^{1*}

(xiaoweil@pennmedicine.upenn.edu)

¹ McKay Orthopaedic Research Laboratory, Department of Orthopaedic Surgery, Perelman School of Medicine, University of Pennsylvania, Philadelphia, PA, United States

² Department of Radiology, Cumming School of Medicine, McCaig Institute for Bone and Joint Health, University of Calgary, Calgary, Canada

Running Title: Predictors of Post-OVX Bone Loss

*To whom correspondence should be addressed X. Sherry Liu
McKay Orthopaedic Research Laboratory
Department of Orthopaedic Surgery
University of Pennsylvania
332A Stemmler Hall, 3450 Hamilton Walk
Philadelphia, PA 19104, USA

Email: xiaoweil@pennmedicine.upenn.edu

Phone: 1-215-746-4668

Conflict of Interest:

The authors declare that they have no conflict of interest.

Number of words in abstract: 274
Number of words in manuscript: 5360
Number of tables: 2
Number of black/white figures: 1
Number of color figures: 2

Abstract:

Postmenopausal osteoporosis affects a large number of women worldwide. Reduced estrogen levels during menopause lead to accelerated bone remodeling, resulting in low bone mass and increased fracture risk. Both peak bone mass and the rate of bone loss are important predictors of postmenopausal osteoporosis risk. However, whether peak bone mass and/or bone microstructure directly influence the rate of bone loss following menopause remains unclear. Our study aimed to establish the relationship between peak bone mass/microstructure and the rate of bone loss in response to estrogen deficiency following ovariectomy (OVX) surgery in rats of homogeneous background by tracking the skeletal changes using in vivo micro-computed tomography (µCT) and three-dimensional (3D) image registrations. Linear regression analyses demonstrated that the peak bone microstructure, but not peak bone mass, was highly predictive of the rate of OVX-induced bone loss. In particular, the baseline trabecular thickness was found to have the highest correlation with the degree of OVX-induced bone loss and trabecular stiffness reduction. Given the same bone mass, the rats with thicker baseline trabeculae had a lower rate of trabecular microstructure and stiffness deterioration after OVX. Moreover, further evaluation to track the changes within each individual trabecula via our novel individual trabecular dynamics (ITD) analysis suggested that a trabecular network with thicker trabeculae is less likely to disconnect or perforate in response to estrogen deficiency, resulting a lower degree of bone loss. Taken together, these findings indicate that the rate of estrogen-deficiency-induced bone loss could be predicted by peak bone microstructure, most notably the trabecular thickness. Given the same bone mass, a trabecular bone phenotype with thin trabeculae may be a risk factor toward accelerated postmenopausal bone loss.

Keywords: Osteoporosis; Ovariectomy; *In vivo* micro-computed tomography; Bone microstructure; Bone mechanical properties; Bone loss predictor

1. Introduction

Postmenopausal osteoporosis is a common metabolic bone disorder that affects approximately 30% of women over the age of 50 in the United States and poses a significant financial burden on healthcare ⁽¹⁻⁴⁾. The rapid decline in estrogen levels during menopause leads to accelerated bone resorption that outpaces bone formation, resulting in skeletal structural deterioration, which subsequently causes bone fragility and elevated fracture risk in postmenopausal women ^(5,6).

Fractures induced by postmenopausal osteoporosis most commonly occur in the spine (vertebral body), hip (femoral neck and intertrochanter), and wrist (distal radius), where trabecular bone predominates (7,8). Trabecular bone has greater surface to volume ratio and considerably greater bone remodeling activities when compared to cortical bone, and thus is more susceptible to loss of bone mass caused by high turnover (9-11). The current gold standard for diagnosing osteoporosis is through assessment of areal bone mineral density (aBMD) using dual-energy X-ray absorptiometry (DXA) (12-14). However, aBMD has significant limitations due to its two-dimensional (2D) nature and its inability to assess bone microstructure. As a result, over 50% of fractures occur in women who are not classified as osteoporotic based on aBMD (15,16). Factors other than aBMD, including three-dimensional (3D) bone density, measured as volumetric bone mineral density (vBMD) and trabecular bone volume fraction (BV/TV), and bone microstructure, such as the orientation, connectivity, and topological types of trabeculae (plate vs. rod) play important roles in maintaining the mechanical integrity of bone (11,17-25). A significant body of work has demonstrated that knowledge of the detailed trabecular microstructure significantly improves fracture risk assessment (19-21).

Despite its substantial burden, osteoporosis is a silently progressing disease, and as a result, is usually not observed until bones have irreversibly weakened and fractures have occurred ⁽²⁶⁾. Therefore, an earlier prediction of osteoporosis risk could contribute to the prevention and management of postmenopausal osteoporosis, and thereby effectively reduce fracture risk. One such factor which can provide an early prediction of postmenopausal osteoporosis risk is the peak bone mass that is attained in young adulthood. A greater bone mass earlier in life provides a buffer so that even in the presence of postmenopausal bone loss, enough bone remains to support the mechanical function of the skeleton ⁽²⁷⁻³¹⁾.

In addition to the peak bone mass and microstructure, the rate of bone loss also plays an important role in predicting osteoporotic fracture risk ⁽³²⁾. A high rate of bone loss postmenopause would lead to rapid deteriorations in bone structure, where bone tissue in unable to accommodate such high remodeling, thereby increasing fracture risk. Indeed, several clinical studies have shown that the annual rate of postmenopausal aBMD change in women who sustained major osteoporotic fractures is significantly higher than those who remained fracture-free ^(33,34). Independent of baseline bone mass, the rate of bone loss may be an additional predictor of fracture risk in postmenopausal women ⁽³⁴⁻³⁷⁾.

Apart from their direct effects on fracture risk, the peak bone mass and postmenopausal bone loss rate also have the potential to interact and influence one another. Thus, peak bone mass and/or bone structure may impact the rate of bone loss following menopause. However, whether or not this occurs remains unclear. Clinical investigations have reported highly variable results on the relationship between baseline BMD and rate of postmenopausal bone loss, ranging from a negative association ⁽³⁸⁾, to no effect ^(39,40), to a positive correlation ⁽⁴¹⁻⁴³⁾ of baseline bone mass with annual rates of bone loss. Several rodent studies compared the skeletal response to estrogen

deficiency induced by ovariectomy (OVX) surgery, which simulated the bone changes observed in women after menopause, among different inbred mouse strains and found that mice with higher initial bone mass (measured as BV/TV) underwent higher rates of bone loss, indicating that higher baseline BV/TV does not necessarily offer protection against estrogen deficiency-induced bone loss (44-46). However, findings of these studies were based on a pool of mice of heterogeneous genetic background. Genetic differences among the mouse strains may act as a confounding factor which influences the peak bone mass as well as the rate of estrogen-deficiency-induced bone loss. Moreover, how peak trabecular bone microstructure, independent of bone mass, affects the rate of estrogen deficiency-induced bone loss remains unclear.

Recent advancements in *in vivo* micro computed tomography (µCT) have enabled OVX-induced changes in 3D bone density and bone microstructure to be longitudinally tracked in rats and mice ⁽⁴⁵⁻⁵³⁾. In a previous study, we tracked skeletal changes following OVX in virgin rats and rats that had previously undergone three cycles of reproduction ⁽⁵⁰⁾. Although the rats with a history of reproduction had drastically less trabecular bone mass prior to OVX, the rate of bone loss in response to OVX was significantly attenuated when compared to age-matched virgin rats. By pooling the data of all rats together, a phenotype of fewer but thicker trabeculae was identified to be protective against OVX-induced bone loss. However, the reproductive history may impact OVX bone loss through other biological pathways, and as a result, the independent effect of peak trabecular bone phenotype on post-OVX bone loss remains unclear. Therefore, the objective of the current study was to investigate the relationship between peak bone mass/microstructure and the rate of bone loss induced by estrogen deficiency in a large cohort of virgin female rats of homogeneous background. In contrast to previous studies in mice and our prior work in post-reproductive rats, where differences in post-OVX bone loss rates may be

driven by outside factors (such as murine strain differences and reproductive history), this study was designed to test whether natural variations in bone microstructure (without external influences) are correlated with post-OVX bone loss rates. This was achieved by tracking skeletal changes using *in vivo* μCT and 3D image registrations. Moreover, our lab has developed a novel image analysis technique, individual trabecular dynamics (ITD) analysis (54), to track the changes of each individual trabecula over time. By applying the ITD analysis, we further elucidated how the thickness of each individual trabecula influences its susceptibility to structural deterioration and bone loss in response to estrogen deficiency. Based on our previous findings, we hypothesized that peak trabecular bone microstructure could play a role in predicting the rate of OVX-induced bone loss.

2. Methods

2.1 Animal Protocol

All animal experiments were approved by the University of Pennsylvania's Institutional Animal Care and Use Committee. A total of 63 female Sprague Dawley rats, purchased from Charles River, underwent bilateral ovariectomy (OVX) surgery at the age of 16-17 weeks followed by osteopenia development for 4 weeks. *In vivo* µCT imaging was performed for all rats prior to OVX and 4 weeks post-OVX. The uterus was collected and weighed immediately post-sacrifice to confirm the success of OVX surgery. Throughout the study, all rats were housed in standard conditions with three rats per cage but were separated to one rat per cage for one week following OVX surgery, followed normal cage activities.

2.2 In Vivo μCT Scans, Image Registration, and Trabecular Bone Microstructural Analysis
 The right proximal tibiae of all rats were imaged using in vivo μCT (Scanco vivaCT40,
 Scanco Medical AG, Brüttisellen, Switzerland) immediately prior to OVX (week 0) and at 4

weeks post-OVX (week 4), following the protocol described in ⁽⁵⁵⁾. Briefly, after μCT calibration, rats were anesthetized (4/2% isoflurane), and the right tibia was fixed in a customized holder to minimize motion. A 4.2 mm thick segment of the proximal tibia, located 0.3 mm below the proximal growth plate, was scanned at 10.5 μm voxel size, with 200 ms integration time, 145 μA current, and 55 kVp energy, resulting in an average scan time of 20 minutes and radiation dose of 0.639 Gy. The *in vivo* μCT image of one rat was excluded in this study due to motion artifacts, resulting in a final sample size of n=62.

Three-dimensional (3D) image registration was performed to longitudinally track changes in trabecular microstructure within a constant trabecular volume of interest (VOI) in the sequential *in vivo* µCT scans of the proximal tibia. Pairs of *in vivo* µCT images for each rat at 0 and 4 weeks post-OVX were aligned by using a mutual-information-based, landmark-initialized, open-source registration toolkit (National Library of Medicine Insight Segmentation and Registration Toolkit) ^(55,56). A 1.5-mm thick, trabecular VOI, located 2 mm distal to the growth plate, was manually segmented in the week 4 scan and traced back to the earlier scan at week 0 based on the transformation matrix that resulted from the registration. Thus, a consistent trabecular VOI of each rat was identified and monitored post-OVX (Fig 1A). Details of the image registration process can be found in our previously published study ⁽⁵⁵⁾.

Standard parameters of trabecular bone microstructure ⁽⁵⁷⁾ were measured within each trabecular VOI. Briefly, the μCT images of trabecular bone were Gaussian filtered (sigma=1.2, support=2) and thresholded by a global threshold (corresponding to 544 mgHA/cm³), identified based on an adaptive threshold function provided by the μCT scanner manufacturer. Trabecular microstructural parameters, such as bone volume fraction (BV/TV), trabecular number (Tb.N), trabecular thickness (Tb.Th), trabecular separation (Tb.Sp), structure model index (SMI), and

connectivity density (Conn.D), were quantified. Percent changes between week 0 and week 4 were calculated for all trabecular parameters in each rat.

2.3 Micro-Finite Element Analysis

Whole-bone stiffness was computed for a 1.5 mm-thick region of the proximal tibia, located 2 mm distal to the growth plate, by using a linear micro-finite element analysis (µFEA) (50). Briefly, the µCT images containing both cortical and trabecular bone compartments were downsampled to a voxel size of 15.75 µm, then each bone voxel was converted to an eight-node brick element, with bone modeled as a linear elastic material with Young's modulus of 15 GPa and Poisson's ratio of 0.3 (58). An axial compression was simulated by applying a displacement of 0.01 mm (1% strain), and the resulting total reaction force was computed (59). In addition, the fraction of the total load carried by the trabecular compartment was calculated at the most distal slice. Based on the trabecular load share fraction, the reaction force exerted by trabecular compartment at the most distal bone slice of the 1.5 mm-thick tibia region was estimated, and applied to calculate the corresponding stiffness of trabecular compartment (Tb.Stiffness) (60).

2.4 Linear Regression Analysis

Martinez-Iglewicz normality test was conducted to test whether the data points could satisfy the assumption underlying the linear regression analysis. Linear regression analysis was applied to investigate the correlations between the baseline (week 0) trabecular microstructural parameters and the corresponding percent changes in trabecular microstructural and mechanical parameters over 4 weeks post-OVX. To evaluate the influence of trabecular bone surface (BS) and bone surface to bone volume ratio (BS/BV) on OVX-induced bone changes, BS and BS/BV were also included in the baseline parameters for linear regression. To further determine the most important factors that predict post-OVX bone loss, a stepwise multiple linear regression was

performed. At each step of the stepwise regression method, the predictors with highest statistical strength entered the model. The stepping ceased when no independent variable reached the standard (p < 0.1) for model entry.

To further determine the independent contribution of baseline trabecular thickness to bone loss regardless of baseline BV/TV, relative Tb.Th was calculated after adjustment by baseline BV/TV using linear regression analysis (Fig 2A-D). Subsequently, all rats were stratified into Low, Medium, and High relative baseline Tb.Th groups, where baseline BV/TV did not differ among the three groups (Fig 2E). Then, the percent changes in trabecular bone volume, structural and mechanical parameters in each relative baseline Tb.Th group were calculated.

2.5 Individual Trabecular Dynamic Analysis

Individual trabecular dynamic (ITD) analysis was performed to longitudinally track the post-OVX changes in volume and connectivity within each individual trabecula, as described in ⁽⁵⁴⁾. Due to the time-consuming nature of this analysis, twenty-four rats were randomly selected. For each rat, a 1.5x1.5x1 mm trabecular subvolume located 2 mm distal to the growth plate was identified, precisely aligned, and thresholded from µCT image pairs made at 0 and 4 weeks post-OVX ^(55,61). The trabecular bone network was then decomposed into individual trabecular plates and rods by using individual trabecular segmentation (ITS) analysis ⁽⁶²⁾ (Figure 3A). By comparing the segmented individual trabecula before and 4 weeks after OVX surgery, the percent change in volume after OVX was quantified. Moreover, changes in connectivity of each individual trabecula over the 4-week period were also examined: connectivity deterioration was defined as a trabecular plate that became perforated or a trabecular rod that disconnected ⁽⁵⁴⁾ (Figure 3A); otherwise, the trabecula was defined as intact. As a result, a total of 11,862

individual trabeculae from the 24 selected rats were analyzed. Additionally, these trabeculae were pooled together and categorized into ten groups based on their thickness prior to OVX, and the percent trabecular bone loss at each thickness was calculated. Moreover, the probability density distributions of baseline trabecular thickness were compared between deteriorated and intact trabeculae.

2.6 Statistical analysis

All results are reported as mean ± standard deviation. Paired Student's T-tests were used to compare trabecular structural parameters as well as whole-bone stiffness between weeks 0 and 4 post-OVX. One-way ANOVA with Bonferroni *post hoc* correction was applied to compare the percent changes in trabecular structural and mechanical properties post-OVX in different trabecular thickness groups. Z-tests were used to compare trabecular thickness distributions between deteriorated and intact trabeculae. For all tests, p-values less than 0.05 were considered statistically significant, while p-values less than 0.1 were considered to indicate a trend of statistical significance with specific p-value provided. In the presence of significant differences, the changes of all parameters, except SMI, are reported as percent difference among different groups. SMI ranges from -3 to 3, thus, inter-group differences in SMI are reported as the absolute difference.

3. Results

3.1 Changes in trabecular microstructure and whole-bone stiffness post-OVX

All rats underwent dramatic trabecular bone loss and structural deterioration post-OVX at the proximal tibia (Fig 1A-G). At 4 weeks post-OVX, BV/TV, Tb.N, Tb.Th, and Conn.D decreased 57%, 39%, 10% and 73%, respectively, as compared to the baseline (week 0). On the other hand, Tb.Sp increased 76% and SMI increased by 1.41 over 4 weeks post-OVX. In

addition to the changes in trabecular bone structure, Tb.Stiffness also decreased 71% over the 4-week post-OVX period (Fig 1H).

3.2 Correlation between baseline trabecular microstructure and degree of post-OVX bone loss

The data points for each parameter were continuous variables with linearity and passed the Martinez-Iglewicz normality test, indicating that the linear regression analysis is an appropriate model to apply. Linear regression analysis was conducted to calculate the correlation coefficients between baseline trabecular parameters and percent changes in trabecular bone microstructural and mechanical properties (Table 1). Surprisingly, no baseline trabecular parameter was significantly correlated to the % decrease in BV/TV, although baseline Tb.Th showed a negative trend of correlation with % decrease in BV/TV (r=-0.21, p=0.097). Moreover, baseline Tb.Th was found to be the best predictor for the % decrease in Conn.D (r=-0.62, p<0.001) and showed a trend of correlation with % decrease in Tb.N (r=-0.23, p=0.069), indicating that greater baseline Tb.Th was associated with reduced loss in BV/TV, Conn.D, and Tb.N. In addition, baseline Conn.D was significantly correlated to % increase in Tb.Sp (r=-0.26, p<0.05). Intriguingly, among all baseline structural parameters, only Tb.Th was correlated with % decrease in Tb.Stiffness, with a correlation coefficient of -0.29 (p<0.05), indicating that greater baseline Tb.Th was associated with reduced post-OVX stiffness deterioration.

As shown in Table 2, stepwise multiple linear regression indicated that the combination of baseline Tb.Th and Conn.D was correlated with % changes in BV/TV, Tb.Sp, and Tb.N, and the combination of baseline Tb.Th, Conn.D, and SMI was highly correlated with % decrease in Conn.D (p<0.01). Moreover, the combination of Tb.Th and Tb.Sp was correlated with % decrease in Tb.Stiffness (p<0.01). Notably, all baseline trabecular structural parameters were

significantly correlated with each other, resulting in multicollinearity when performing multiple linear regression analyses (Supplemental Table 1).

3.3 Effects of baseline Tb.Th on OVX-induced bone loss

To further examine the influence of baseline Tb.Th independent of baseline BV/TV on OVX-induced bone loss, all data were divided into three tertiles based on relative baseline Tb.Th after adjustment of baseline BV/TV (Fig 2 A-D). Linear regression analysis revealed that the baseline Tb.Th was highly correlated with the baseline BV/TV (r=0.87, p<0.001; Fig 2D), and the corresponding residuals were used to stratify rats into Low, Medium, and High relative baseline Tb.Th groups. As a result of this classification scheme, there was no difference in the baseline BV/TV among these three relative Tb.Th groups (Fig 2E). However, substantial variations in baseline Tb.Th were shown among the Low, Medium, and High relative Tb.Th groups (Fig 2A-C), where rats in the High relative Tb.Th group showed 13% greater baseline Tb.Th, as compared to the Low relative Tb.Th group (Fig 2F). Comparison of post-OVX bone loss patterns among the groups indicated that the % decrease in BV/TV was 15% lower in the High compared to the Low relative Tb.Th group (Fig 2G), and the % decrease in Conn.D in the High group was 15% and 10% lower than the Low and Medium groups, respectively (Fig 2H). Similar results were found for % decrease in Tb.N and % increase in Tb.Sp (Fig 2IJ), but no inter-group differences were found in % decrease in Tb.Th (Fig 2K). Furthermore, % decrease in Tb.Stiffness was 13% lower in the High compared to the Low relative Tb.Th group (Fig 2L). Thus, given the same baseline BV/TV, rats with greater baseline Tb.Th underwent attenuated loss in the volume, number, connectivity, and stiffness of the trabecular bone network and reduced expansion in the spacing between trabeculae, but did not show differences in the loss in thickness of trabeculae induced by OVX.

3.4 Effects of baseline Tb.Th on structural deterioration in individual trabeculae

A total of 11,862 individual trabeculae were tracked over the 4 weeks post-OVX. When trabeculae were categorized to ten groups based on their baseline Tb.Th, intriguing patterns of post-OVX bone loss became apparent. Comparisons of the percentage of bone loss among trabeculae with different baseline thicknesses showed significant differences between adjacent thickness groups when the baseline thickness was in the range of 0.03-0.08mm, indicating that, within this range, trabeculae with greater baseline thickness had a reduced percentage bone loss. Meanwhile, no difference between adjacent bins was found when the baseline thickness is outside of the range (less than 0.03 mm or greater than 0.08mm, Fig 3B). Thus, the effect of trabecular thickness on OVX-induced bone loss appeared to initialize when trabecular thickness was greater than 0.03 mm, and plateau for thicknesses above 0.08 mm.

Evaluation of structural deterioration of the trabeculae indicated that a total of 3,311 trabeculae underwent rod disconnection or plate perforation, and 8,405 remained intact after OVX. Gaussian curves fitted to the trabecular thickness distribution of deteriorated (rod disconnected or plate perforated) and intact trabeculae (Fig 3C) indicated that the trabeculae whose structure deteriorated after OVX had 16% lower baseline trabecular thickness than those that remained intact.

4. Discussion

This study investigated the relationship between the peak trabecular bone mass/microstructure and the rate of estrogen deficiency-induced bone loss in a homogeneous background of virgin female Sprague Dawley rats. Overall, the results indicate that the peak bone microstructure attained prior to OVX is highly predictive of the rate of OVX bone loss. In particular, the baseline Tb.Th was found to have the highest correlation with the degree of OVX

bone loss and is considered the most important predictor of the rate of estrogen-deficiencyinduced bone loss and connectivity deterioration.

As expected, estrogen deficiency induced substantial trabecular bone loss and microstructural deterioration over the 4-week post-OVX period in all rats. Although rats show continuous longitudinal growth throughout their lifespan, the growth rate of long bone significantly slow down at the age of 3 months (63), and, in accordance to our previous studies, no significant age-related change in trabecular microstructure was detected in the proximal tibia from age 16-17 weeks to 21-22 weeks (64), indicating that the dramatic tibial trabecular bone loss and microstructural deterioration found in this current study were induced by OVX surgery. These findings align with several previous in vivo µCT-based studies in which a significant deterioration in trabecular microarchitecture was observed at the rat proximal tibia following OVX surgery (48,50,53,65). As osteoporosis progresses, the thickness and number of trabeculae significantly reduce, and, as a result of microstructural deterioration, the topological type of trabeculae shifts from plate-like to rod-like structure. The elevated remodeling of individual trabecula induced by OVX causes disconnection of the trabecular bone network and increased separation between trabeculae. An important body of work has demonstrated that this trabecular phenotype is associated with decreased mechanical competence and increased fracture risk (66,67).

This study provides new insight on the pathophysiology of osteoporotic bone loss by seeking to correlate microstructural parameters with bone loss rates. Based on the linear regression analyses, we found no correlation between baseline bone mass and the rate of OVX-induced bone loss. However, in contrast to our current findings, our previous study, which tracked skeletal changes following OVX in virgin rats and rats with reproductive history, found a positive correlation between baseline bone mass and the degree of post-OVX bone loss when

pooling the data of all rats together ⁽⁵⁰⁾. However, the reproductive history may impact OVX bone loss through other biological pathways, and as a result, the independent effects of peak trabecular bone mass on the rate of post-OVX bone loss could not be isolated in a cohort of virgin and reproductive rats with heterogeneous background. Similarly, studies in mice with heterogeneous genetic background also found a positive correlation between OVX-induced bone loss and baseline bone mass at the proximal tibia ^(45,46). Since different mouse strains were utilized in these studies to compare the rate of bone loss caused by OVX, the positive correlation between baseline bone mass and OVX bone loss rate may be partially attributed to the genetic heterogeneity of the mice. Indeed, when each mouse strain was considered independently, no significant correlations were detected between baseline BV/TV and the extent of post-OVX bone loss ⁽⁴⁵⁾, which is consistent with our current results.

Moreover, previous clinical investigations provide highly variable information on the association between peak bone mass and postmenopausal bone loss rate. Some clinical studies suggested that the baseline trabecular vBMD could not predict the rate of bone loss by pQCT measurements at the distal radius in peri- and postmenopausal women ⁽³⁹⁾. Moreover, a recent study showed that the peak aBMD and the rate of bone loss during early postmenopause assessed by DXA at lumbar spine are independent risk factors for subsequent fractures ⁽⁴⁰⁾. However, contrary to our findings, other data suggested that women with lower peak bone mass may undergo a higher rate of bone loss based on forearm measurements by pQCT imaging ⁽³⁸⁾, while others found opposite results by femoral neck DXA measurements that women with higher baseline aBMD have greater rate of bone loss ⁽⁴¹⁻⁴³⁾. These inconsistent observations could be caused mainly by two reasons: 1) differences in measurement technique: DXA-based aBMD is influenced by bone size and cannot distinguish between cortical and trabecular bone, which may

Variations in study designs, measured bone sites (weight-bearing site *vs.* non-weight-bearing site), timing of the longitudinal CT measurements (at pre-, peri-, or during menopause), and population characteristics (racial, social, and cultural confounding factors) may also impact their results and conclusions. Therefore, taken all together, standard measurement of peak bone mass by DXA may not be a reliable predictor of bone loss rate post menopause.

The peak bone microstructure may provide further insight in predicting the rate of postmenopausal bone loss. One clinical measure of trabecular bone quality, the trabecular bone score (TBS), provides an indirect measurement of trabecular microstructure by evaluating the texture of lumbar spine DXA images ⁽⁶⁸⁾. A recent study found that a low baseline TBS (indicative of a deteriorated trabecular microstructure) was associated with a higher percentage of bone loss and osteoporosis at follow-up in perimenopausal women ⁽⁶⁹⁾, indicating that the peak bone microstructure may have the potential to predict the rate of bone loss when subjected to estrogen deficiency.

Our current findings indicate that, among all baseline trabecular microstructural parameters, only baseline trabecular thickness showed a negative trend of correlation with OVX-induced bone loss rate by linear regression. Moreover, stepwise multiple linear regression analysis confirmed that the combination of baseline Tb.Th and Conn.D are the most important predictors for the extent of post-OVX bone loss. While there was a positive association between baseline Conn.D and the degree of OVX bone loss, the baseline Tb.Th was correlated inversely, suggesting that a trabecular bone phenotype with thicker trabeculae and fewer connections are protective against OVX bone loss. Surprisingly, we found no correlation between baseline trabecular surface area and the rate of post-OVX bone loss, and thus, the protective effect of

increased Tb.Th on post-OVX bone loss appears to be independent of any possible relationship to remodeling surface area.

Indeed, the results from the tertile analysis of Tb.Th adjusted by baseline BV/TV suggest that given the same bone mass (baseline BV/TV), rats with thicker trabeculae had attenuated reduction in volume, number, and connectivity of trabeculae and greater increase in spacing between trabeculae in response to OVX, suggesting that thicker trabeculae were associated with greater resistance to loss of trabecular network integrity. In contrast, rates of post-OVX trabecular thickness loss were similar among all 3 tertiles, suggesting a similar level of trabecular thinning regardless of their baseline thickness. Overall, the improved resistance of thicker trabeculae to post-OVX microstructural decay resulted in a protective effect against loss of trabecular bone stiffness.

Consistent with these findings, our previous study found that the thicker trabeculae attained in rats with a history of lactation are significantly associated with attenuated OVX-induced bone loss compared to the age-matched virgin rats (50). Moreover, despite the distinct bone loss patterns between the two groups, the number and surface of osteoblasts and osteoclasts post-OVX did not differ between virgin rats and rats with a history of lactation. Furthermore, it has been shown that OVX-induced bone loss is more likely to progress through diminished connectivity than a gradual thinning of overall trabeculae (45). Similar mechanisms are thought to occur post-menopause: the trabecular elements that perforate or disconnect post-menopause lead to deteriorated connectivity in the trabecular network, thus resulting in an accelerated bone loss (70-72). Along with our current and previous results that thicker trabeculae resulted in attenuated bone deterioration post-OVX (50), these findings suggest that thicker trabeculae may be protective against structural deterioration in response to estrogen deficiency. Our working hypothesis is that

the increased bone remodeling due to estrogen deficiency has varied effects on the structural integrity of the trabecular network depending on the trabecular thickness. For thick trabeculae, the bone resorption occurring post-OVX can be repaired by subsequent osteoblast activities (Fig. 3D). However, the thin trabeculae may easily disconnect during the rapid remodeling phase and cannot be repaired afterwards (Fig 3E). Indeed, the results from ITD analyses demonstrated a "thickness effect" in which a trabecular network with thicker individual trabeculae is less likely to be disconnected or perforated post-OVX, which leads to attenuated OVX bone loss. Intriguingly, our results suggested that this "thickness effect" would initialize at trabecular thicknesses greater than 0.03 mm, and plateau at thicknesses beyond 0.08 mm. Therefore, it is possible that 0.03 mm is a lower limit for the "thickness effect", as all the individual trabeculae thinner than the lower limit may always be perforated or separated due to the rapid bone resorption post-OVX; and conversely, 0.08 mm could be considered as an upper limit for the "thickness effect", as the extent of post-OVX bone remodeling may not be enough to induce any perforation or separation in trabeculae with baseline thickness beyond this upper limit. As reported by previous studies, the average depth of osteoclast resorption cavities varies between 0.014 and 0.063 mm ^(73,74), which is consistent with the upper and lower thickness limits demonstrated by the current study. Defining the lower and upper thickness limits in a clinical setting could yield a better understanding and prediction of post-menopausal bone loss, as they likely define the susceptibility of trabeculae of various thickness to structural deterioration and elevated bone loss.

Evaluation of the relationship between baseline trabecular microstructure and OVX-induced changes in trabecular stiffness (estimated through FEA) indicated that only baseline trabecular thickness was significantly and negatively correlated with OVX-induced changes in

trabecular stiffness, Moreover, tertile analyses revealed that regardless of the baseline trabecular bone volume, rats with thicker trabeculae underwent attenuated reduction in the stiffness of the trabecular compartment post-OVX, which further suggests that a trabecular bone phenotype with thicker baseline trabeculae may better preserve its mechanical integrity when subjected to estrogen deficiency, and thus, reducing the fracture risk post-menopause.

Our study has some limitations. First, biochemical markers of bone remodeling or histomorphometry were not assessed, therefore it is not possible to directly compare the bone cell activities among rats with variable peak bone microstructure. Whether or not the baseline bone microstructure has influence on the bone remodeling rate post-OVX is not clear and requires further investigation. Moreover, in contrast to the high similarities in trabecular bone compartments between rats and humans, humans have distinct cortical bone remodeling than rats. In humans, the increased Haversian remodeling post-menopause exerts a main contribution to cortical porosity, while rats lack a well-developed Haversian remodeling system, and a result, rats cannot mimic the changes in human cortical bone post-menopause (75). Thirdly, the voxel size of the μCT scans was 10.5μm, limiting the power of *in vivo* μCT scans in detecting small changes over time. However, it has been suggested that by applying the current settings of scanning (e.g. additional fixation to the scanned sites) and post-scanning image processing of 3D registration, the *in vivo* μCT measurements yielded a reasonable precision in detecting changes in rodent trabecular bone (55). Lastly, only one time point (4 weeks post-OVX) was measured, and thus our conclusions are limited to early post-OVX bone loss. Evaluation of an extended post-OVX duration in future work is warranted to further elucidate the impact of peak bone microstructure on post-OVX bone changes.

Despite these shortcomings, our study provides relevant and novel insight into predicting

early onset of postmenopausal osteoporosis using a gold standard rat model. Although the implications for translating these findings to clinical remain to be confirmed, the similarities of hormonal changes and skeletal responses between OVX rats and postmenopausal women are well established ⁽⁷⁶⁾. To our knowledge, this study represents the first attempt to establish a relationship between peak trabecular parameters and the degree of OVX-induced bone loss in individual trabeculae in a homogeneous rodent population. The state-of-art imaging technologies used in this study allowed us to accurately track and monitor *in vivo* bone structural changes at an individual trabecula level. Moreover, utilizing ITD analysis, the influence of the thickness of each individual trabecula on its susceptibility to disconnection or perforation in response to elevated rate of bone remodeling was elucidated.

In summary, the extent of estrogen-deficiency-induced bone loss was predicted by peak bone microarchitecture, most notably the trabecular thickness. Specifically, trabecular networks with thick trabeculae showed an attenuation in OVX-induced trabecular bone microstructure and stiffness deterioration. Further analysis suggests that thicker trabeculae are less likely to be disconnected or perforated in response to estrogen deficiency, as the resorbed bone is more likely to be repaired by the coupled bone formation. Taken together, these findings suggest that given the same bone mass, a trabecular bone phenotype with thin trabeculae may be a risk factor toward accelerated postmenopausal bone loss, which provides important clinical insights toward the development of patient-specific osteoporosis management strategies based on peak bone microstructure.

5. Acknowledgements

Research reported in this publication was supported by the Penn Center for Musculoskeletal Diseases (PCMD) NIH/NIAMS P30-AR069619, NIH/NIAMS K01-AR066743

(to XSL), NIH/NIAMS R01-AR071718 (to XSL), and National Science Foundation (NSF) Award #1653216 (to XSL).

6. Author's roles:

Study design: XSL, YL. Study conduct: YL, WJT, CMJdB, HZ. Data collection and analysis: YL, WJT, HZ. Data interpretation: XSL, YL. Drafting manuscript: YL. Revising manuscript content: XSL, CMJdB, RC. Approving final version of manuscript: XSL, YL, WJT, CMJdB, HZ, RC. XSL and YL take responsibility for the integrity of the data analysis.

References:

- 1. Kanis JA, Melton III LJ, Christiansen C, Johnston CC, Khaltaev N. The diagnosis of osteoporosis. Journal of bone and mineral research. 1994;9(8):1137-41.
- 2. Health UDo, Services H. Bone health and osteoporosis: a report of the Surgeon General. Rockville, MD: US Department of Health and Human Services, Office of the Surgeon General. 2004;87.
- 3. Lane NE. Epidemiology, etiology, and diagnosis of osteoporosis. American journal of obstetrics and gynecology. Feb 2006;194(2 Suppl):S3-11.
- 4. Wright NC, Saag KG, Dawson-Hughes B, Khosla S, Siris ES. The impact of the new National Bone Health Alliance (NBHA) diagnostic criteria on the prevalence of osteoporosis in the USA. Osteoporosis international: a journal established as result of cooperation between the European Foundation for Osteoporosis and the National Osteoporosis Foundation of the USA. Apr 2017;28(4):1225-32.
- 5. Bouillon R, Burckhardt P, Christiansen C, Fleisch H, Fujita T, Gennari C, et al. Consensus development conference: prophylaxis and treatment of osteoporosis. Am J Med. 1991;90:107-10.
- 6. Meunier PJ, Delmas PD, Eastell R, McClung MR, Papapoulos S, Rizzoli R, et al. Diagnosis and management of osteoporosis in postmenopausal women: clinical guidelines. International Committee for Osteoporosis Clinical Guidelines. Clinical therapeutics. Jun 1999;21(6):1025-44.
- 7. National CGCU. Osteoporosis: Fragility Fracture Risk: Osteoporosis: Assessing the Risk of Fragility Fracture. 2012.
- 8. Burge R, Dawson-Hughes B, Solomon DH, Wong JB, King A, Tosteson A. Incidence and economic burden of osteoporosis-related fractures in the United States, 2005-2025. Journal of bone and mineral research: the official journal of the American Society for Bone and Mineral Research. Mar 2007;22(3):465-75.
- 9. Parfitt AM. Osteonal and hemi-osteonal remodeling: the spatial and temporal framework for signal traffic in adult human bone. Journal of cellular biochemistry. 1994;55(3):273-86
- 10. Parfitt AM. Trabecular bone architecture in the pathogenesis and prevention of fracture. The American journal of medicine. 1987;82(1):68-72.
- 11. Oftadeh R, Perez-Viloria M, Villa-Camacho JC, Vaziri A, Nazarian A. Biomechanics and mechanobiology of trabecular bone: a review. Journal of biomechanical engineering. 2015;137(1):010802.
- 12. Kleerekoper M, Nelson DA. Which bone density measurement? Journal of bone and mineral research: the official journal of the American Society for Bone and Mineral Research. May 1997;12(5):712-4.
- 13. Osterhoff G, Morgan EF, Shefelbine SJ, Karim L, McNamara LM, Augat P. Bone mechanical properties and changes with osteoporosis. Injury. Jun 2016;47 Suppl 2:S11-20.
- 14. Miller PD, Leonard MB. Clinical use of bone mass measurements in adults for the assessment and management of osteoporosis. Primer on the Metabolic Bone Disease and Disorders of Mineral Metabolism, 6th ed, American Society for Bone and Mineral Research, Washington, DC. 2006:150-61.

- 15. Stone KL, Seeley DG, Lui LY, Cauley JA, Ensrud K, Browner WS, et al. BMD at multiple sites and risk of fracture of multiple types: long-term results from the Study of Osteoporotic Fractures. Journal of bone and mineral research: the official journal of the American Society for Bone and Mineral Research. Nov 2003;18(11):1947-54.
- 16. Schuit S, Van der Klift M, Weel A, De Laet C, Burger H, Seeman E, et al. Fracture incidence and association with bone mineral density in elderly men and women: the Rotterdam Study. Bone. 2004;34(1):195-202.
- 17. Keaveny TM, Morgan EF, Niebur GL, Yeh OC. Biomechanics of trabecular bone. Annu Rev Biomed Eng. 2001;3:307-33.
- 18. Bouxsein ML. Bone quality: where do we go from here? Osteoporosis international. 2003;14(5):118-27.
- 19. de Bakker CMJ, Tseng WJ, Li Y, Zhao H, Liu XS. Clinical Evaluation of Bone Strength and Fracture Risk. Current osteoporosis reports. Feb 2017;15(1):32-42.
- 20. Nishiyama KK, Shane E. Clinical imaging of bone microarchitecture with HR-pQCT. Current osteoporosis reports. Jun 2013;11(2):147-55.
- 21. Cheung AM, Adachi JD, Hanley DA, Kendler DL, Davison KS, Josse R, et al. High-resolution peripheral quantitative computed tomography for the assessment of bone strength and structure: a review by the Canadian Bone Strength Working Group. Current osteoporosis reports. Jun 2013;11(2):136-46.
- 22. Jensen K, Mosekilde L, Mosekilde L. A model of vertebral trabecular bone architecture and its mechanical properties. Bone. 1990;11(6):417-23.
- 23. Liu XS, Sajda P, Saha PK, Wehrli FW, Guo XE. Quantification of the roles of trabecular microarchitecture and trabecular type in determining the elastic modulus of human trabecular bone. Journal of bone and mineral research: the official journal of the American Society for Bone and Mineral Research. Oct 2006;21(10):1608-17.
- 24. Stauber M, Rapillard L, van Lenthe GH, Zysset P, Muller R. Importance of individual rods and plates in the assessment of bone quality and their contribution to bone stiffness. Journal of bone and mineral research: the official journal of the American Society for Bone and Mineral Research. Apr 2006;21(4):586-95.
- 25. Nazarian A, Muller J, Zurakowski D, Muller R, Snyder BD. Densitometric, morphometric and mechanical distributions in the human proximal femur. Journal of biomechanics. 2007;40(11):2573-9.
- 26. Arceo-Mendoza RM, Camacho P. Prediction of fracture risk in patients with osteoporosis: a brief review. Women's health. 2015;11(4):477-84.
- 27. Bonjour JP, Chevalley T, Ferrari S, Rizzoli R. The importance and relevance of peak bone mass in the prevalence of osteoporosis. Salud publica de Mexico. 2009;51 Suppl 1:S5-17.
- 28. Newton-John H, Morgan DB. 27 The Loss of Bone with Age, Osteoporosis, and Fractures. Clinical Orthopaedics and Related Research®. 1970;71:229-52.
- 29. Emaus N, Berntsen GK, Joakimsen R, Fonnebo V. Longitudinal changes in forearm bone mineral density in women and men aged 45-84 years: the Tromso Study, a population-based study. American journal of epidemiology. Mar 1 2006;163(5):441-9. Epub 2006/01/06.
- 30. Loro ML, Sayre J, Roe TF, Goran MI, Kaufman FR, Gilsanz V. Early identification of children predisposed to low peak bone mass and osteoporosis later in life. The Journal of clinical endocrinology and metabolism. Oct 2000;85(10):3908-18.

- 31. Melton LJ, 3rd, Atkinson EJ, Khosla S, Oberg AL, Riggs BL. Evaluation of a prediction model for long-term fracture risk. Journal of bone and mineral research: the official journal of the American Society for Bone and Mineral Research. Apr 2005;20(4):551-6.
- 32. Papaioannou A, Morin S, Cheung AM, Atkinson S, Brown JP, Feldman S, et al. 2010 clinical practice guidelines for the diagnosis and management of osteoporosis in Canada: summary. Cmaj. 2010;182(17):1864-73.
- 33. Riis BJ, Hansen MA, Jensen AM, Overgaard K, Christiansen C. Low bone mass and fast rate of bone loss at menopause: equal risk factors for future fracture: a 15-year follow-up study. Bone. Jul 1996;19(1):9-12.
- 34. Nguyen TV, Center JR, Eisman JA. Femoral neck bone loss predicts fracture risk independent of baseline BMD. Journal of bone and mineral research: the official journal of the American Society for Bone and Mineral Research. Jul 2005;20(7):1195-201.
- 35. Berger C, Langsetmo L, Joseph L, Hanley DA, Davison KS, Josse RG, et al. Association between change in BMD and fragility fracture in women and men. Journal of bone and mineral research: the official journal of the American Society for Bone and Mineral Research. Feb 2009;24(2):361-70.
- 36. Hillier TA, Stone KL, Bauer DC, Rizzo JH, Pedula KL, Cauley JA, et al. Evaluating the value of repeat bone mineral density measurement and prediction of fractures in older women: the study of osteoporotic fractures. Arch Intern Med. Jan 22 2007;167(2):155-60.
- 37. Ahmed LA, Emaus N, Berntsen GK, Bjornerem A, Fonnebo V, Jorgensen L, et al. Bone loss and the risk of non-vertebral fractures in women and men: the Tromso study. Osteoporosis international: a journal established as result of cooperation between the European Foundation for Osteoporosis and the National Osteoporosis Foundation of the USA. Sep 2010;21(9):1503-11.
- 38. Radspieler H, Dambacher MA, Kissling R, Neff M. Is the amount of trabecular bone-loss dependent on bone mineral Density? A study performed by three centres of osteoporosis using high resolution peripheral quantitative computed tomography. Eur J Med Res. Jan 26 2000;5(1):32-9.
- 39. Qin L, Au SK, Leung PC, Lau MC, Woo J, Choy WY, et al. Baseline BMD and bone loss at distal radius measured by peripheral quantitative computed tomography in periand postmenopausal Hong Kong Chinese women. Osteoporosis international: a journal established as result of cooperation between the European Foundation for Osteoporosis and the National Osteoporosis Foundation of the USA. Dec 2002;13(12):962-70.
- 40. Albert Shieh AK, Mei-Hua Huang, Weijuan Han, Gail Greendale. The associations of peak bone mineral density and rate of bone mineral density loss during the menopause transition and early postmenopause with subsequent fracture: results from the Study of Women's Health Across the Nation (SWAN). in American Society of Bone and Mineral Research Annual Meeting. 2020.
- 41. Davis JW, Grove JS, Ross PD, Vogel JM, Wasnich RD. Relationship between bone mass and rates of bone change at appendicular measurement sites. Journal of bone and mineral research: the official journal of the American Society for Bone and Mineral Research. Jul 1992;7(7):719-25. Epub 1992/07/01.
- 42. Bainbridge KE, Sowers MF, Crutchfield M, Lin X, Jannausch M, Harlow SD. Natural history of bone loss over 6 years among premenopausal and early postmenopausal women. American journal of epidemiology. Sep 1 2002;156(5):410-7.

- 43. Melton LJ, 3rd, Atkinson EJ, O'Connor MK, O'Fallon WM, Riggs BL. Determinants of bone loss from the femoral neck in women of different ages. Journal of bone and mineral research: the official journal of the American Society for Bone and Mineral Research. Jan 2000;15(1):24-31.
- 44. Bouxsein ML, Myers KS, Shultz KL, Donahue LR, Rosen CJ, Beamer WG. Ovariectomy-induced bone loss varies among inbred strains of mice. Journal of bone and mineral research: the official journal of the American Society for Bone and Mineral Research. Jul 2005;20(7):1085-92.
- 45. Klinck J, Boyd SK. The magnitude and rate of bone loss in ovariectomized mice differs among inbred strains as determined by longitudinal in vivo micro-computed tomography. Calcified tissue international. Jul 2008;83(1):70-9.
- 46. Farooq S, Leussink S, Sparrow LM, Marchini M, Britz HM, Manske SL, et al. Cortical and trabecular morphology is altered in the limb bones of mice artificially selected for faster skeletal growth. Sci Rep. Sep 5 2017;7(1):10527.
- 47. Waarsing JH, Day JS, van der Linden JC, Ederveen AG, Spanjers C, De Clerck N, et al. Detecting and tracking local changes in the tibiae of individual rats: a novel method to analyse longitudinal in vivo micro-CT data. Bone. Jan 2004;34(1):163-9.
- 48. Boyd SK, Davison P, Muller R, Gasser JA. Monitoring individual morphological changes over time in ovariectomized rats by in vivo micro-computed tomography. Bone. Oct 2006;39(4):854-62.
- 49. Campbell GM, Buie HR, Boyd SK. Signs of irreversible architectural changes occur early in the development of experimental osteoporosis as assessed by in vivo micro-CT. Osteoporosis international: a journal established as result of cooperation between the European Foundation for Osteoporosis and the National Osteoporosis Foundation of the USA. Oct 2008;19(10):1409-19.
- 50. de Bakker CM, Li Y, Zhao H, Leavitt L, Tseng WJ, Lin T, et al. Structural Adaptations in the Rat Tibia Bone Induced by Pregnancy and Lactation Confer Protective Effects Against Future Estrogen Deficiency. Journal of bone and mineral research: the official journal of the American Society for Bone and Mineral Research. Jul 24 2018. Epub 2018/07/25.
- 51. Klinck RJ, Campbell GM, Boyd SK. Radiation effects on bone architecture in mice and rats resulting from in vivo micro-computed tomography scanning. Med Eng Phys. Sep 2008;30(7):888-95.
- 52. Roberts BC, Giorgi M, Oliviero S, Wang N, Boudiffa M, Dall'Ara E. The longitudinal effects of ovariectomy on the morphometric, densitometric and mechanical properties in the murine tibia: A comparison between two mouse strains. Bone. Oct 2019;127:260-70.
- 53. Altman-Singles AR, Jeong Y, Tseng WJ, de Bakker CM, Zhao H, Lott C, et al. Intermittent Parathyroid Hormone After Prolonged Alendronate Treatment Induces Substantial New Bone Formation and Increases Bone Tissue Heterogeneity in Ovariectomized Rats. Journal of bone and mineral research: the official journal of the American Society for Bone and Mineral Research. Aug 2017;32(8):1703-15. Epub 2017/05/04.
- 54. Altman AR, de Bakker CM, Tseng WJ, Chandra A, Qin L, Liu XS. Enhanced individual trabecular repair and its mechanical implications in parathyroid hormone and alendronate treated rat tibial bone. Journal of biomechanical engineering. Jan 2015;137(1).

- 55. Lan S, Luo S, Huh BK, Chandra A, Altman AR, Qin L, et al. 3D image registration is critical to ensure accurate detection of longitudinal changes in trabecular bone density, microstructure, and stiffness measurements in rat tibiae by in vivo microcomputed tomography (muCT). Bone. Sep 2013;56(1):83-90.
- 56. Johnson HJ, McCormick M, Ibanez L. The itk software guide third edition updated for itk version 4.5. Insight Software Consortium, Tech rep. 2013.
- 57. Bouxsein ML, Boyd SK, Christiansen BA, Guldberg RE, Jepsen KJ, Muller R. Guidelines for assessment of bone microstructure in rodents using micro-computed tomography. Journal of bone and mineral research: the official journal of the American Society for Bone and Mineral Research. Jul 2010;25(7):1468-86. Epub 2010/06/10.
- 58. Guo XE, Liang LC, Goldstein SA. Micromechanics of osteonal cortical bone fracture. Journal of biomechanical engineering. Feb 1998;120(1):112-7. Epub 1998/07/24.
- 59. Hollister SJ, Brennan JM, Kikuchi N. A homogenization sampling procedure for calculating trabecular bone effective stiffness and tissue level stress. Journal of biomechanics. Apr 1994;27(4):433-44. Epub 1994/04/01.
- 60. de Bakker CMJ, Tseng WJ, Li Y, Zhao H, Altman-Singles AR, Jeong Y, et al. Reproduction Differentially Affects Trabecular Bone Depending on Its Mechanical Versus Metabolic Role. Journal of biomechanical engineering. Nov 1 2017;139(11).
- de Bakker CM, Altman AR, Tseng WJ, Tribble MB, Li C, Chandra A, et al. muCT-based, in vivo dynamic bone histomorphometry allows 3D evaluation of the early responses of bone resorption and formation to PTH and alendronate combination therapy. Bone. Apr 2015;73:198-207. Epub 2015/01/03.
- 62. Liu XS, Sajda P, Saha PK, Wehrli FW, Bevill G, Keaveny TM, et al. Complete volumetric decomposition of individual trabecular plates and rods and its morphological correlations with anisotropic elastic moduli in human trabecular bone. Journal of bone and mineral research: the official journal of the American Society for Bone and Mineral Research. Feb 2008;23(2):223-35.
- 63. Altman AR, Tseng WJ, de Bakker CMJ, Chandra A, Lan S, Huh BK, et al. Quantification of skeletal growth, modeling, and remodeling by in vivo micro computed tomography. Bone. Dec 2015;81:370-9.
- de Bakker CM, Altman-Singles AR, Li Y, Tseng WJ, Li C, Liu XS. Adaptations in the Microarchitecture and Load Distribution of Maternal Cortical and Trabecular Bone in Response to Multiple Reproductive Cycles in Rats. Journal of bone and mineral research: the official journal of the American Society for Bone and Mineral Research. May 2017;32(5):1014-26.
- 65. Waarsing JH, Day JS, Verhaar JA, Ederveen AG, Weinans H. Bone loss dynamics result in trabecular alignment in aging and ovariectomized rats. Journal of orthopaedic research : official publication of the Orthopaedic Research Society. May 2006;24(5):926-35. Epub 2006/04/04.
- 66. Karlamangla AS, Burnett-Bowie SM, Crandall CJ. Bone Health During the Menopause Transition and Beyond. Obstet Gynecol Clin North Am. Dec 2018;45(4):695-708.
- 67. Samelson EJ, Broe KE, Xu H, Yang L, Boyd S, Biver E, et al. Cortical and trabecular bone microarchitecture as an independent predictor of incident fracture risk in older women and men in the Bone Microarchitecture International Consortium (BoMIC): a prospective study. Lancet Diabetes Endocrinol. Jan 2019;7(1):34-43.

- 68. Silva BC, Leslie WD, Resch H, Lamy O, Lesnyak O, Binkley N, et al. Trabecular bone score: a noninvasive analytical method based upon the DXA image. Journal of bone and mineral research: the official journal of the American Society for Bone and Mineral Research. Mar 2014;29(3):518-30.
- 69. Gutierrez-Buey G, Restituto P, Botella S, Monreal I, Colina I, Rodriguez-Fraile M, et al. Trabecular bone score and bone remodelling markers identify perimenopausal women at high risk of bone loss. Clin Endocrinol (Oxf). Sep 2019;91(3):391-9.
- 70. Liu XS, Huang AH, Zhang XH, Sajda P, Ji B, Guo XE. Dynamic simulation of three dimensional architectural and mechanical alterations in human trabecular bone during menopause. Bone. Aug 2008;43(2):292-301. Epub 2008/06/14.
- 71. Chen H, Zhou X, Fujita H, Onozuka M, Kubo KY. Age-related changes in trabecular and cortical bone microstructure. International journal of endocrinology. 2013;2013:213234. Epub 2013/04/11.
- 72. Eriksen EF. Normal and pathological remodeling of human trabecular bone: three dimensional reconstruction of the remodeling sequence in normals and in metabolic bone disease. Endocrine reviews. Nov 1986;7(4):379-408. Epub 1986/11/01.
- 73. Bain SD, Gross TS. Structural Aspects of Bone Resorption. In: Bronner F, Farach-Carson MC, Rubin J, editors. Bone Resorption. London: Springer London; 2005. p. 58-66.
- 74. Slyfield CR, Tkachenko EV, Wilson DL, Hernandez CJ. Three-dimensional dynamic bone histomorphometry. Journal of bone and mineral research: the official journal of the American Society for Bone and Mineral Research. Feb 2012;27(2):486-95.
- 75. Lelovas PP, Xanthos TT, Thoma SE, Lyritis GP, Dontas IA. The laboratory rat as an animal model for osteoporosis research. Comp Med. Oct 2008;58(5):424-30.
- 76. Kalu DN. The ovariectomized rat model of postmenopausal bone loss. Bone and mineral. Dec 1991;15(3):175-91. Epub 1991/12/01.

Table 1: Correlation coefficients (r) between baseline trabecular parameters and % decrease in trabecular microstructural and mechanical properties

% decrease *	Baseline Parameters								
	BV/TV	Conn.D	SMI	Tb.N	Tb.Th	Tb.Sp	BS	BS/BV	
BV/TV	NS	NS	NS	NS	-0.21 (p=0.097)	NS	NS	NS	
Tb.Th	0.64 ^c	0.50 °	-0.62 °	0.57 °	0.62 °	-0.57 ^c	0.43 ^c	-0.66 ^c	
Tb.Sp	NS	-0.26 a	NS	NS	NS	NS	NS	NS	
Tb.N	NS	NS	NS	NS	-0.23 (p=0.069)	NS	NS	NS	
Conn.D	-0.46 b	NS	0.49 b	-0.26 a	-0.62 °	0.26 a	NS	0.57 °	
Tb.Stiffness	NS	NS	NS	NS	-0.29 a	NS	NS	NS	

^{*:} Baseline parameters were correlated to percent decrease in all parameters for consistency. For the parameters that increased after OVX surgery (Tb.Sp), the percent decrease means a negative decrease.

Minus sign indicates negative correlation. a: p<0.05, b: p<0.01, c: p<0.001.

Table 2: Correlation coefficients (r) and independent predictors of stepwise multiple linear regression to predict the degree of bone loss by baseline trabecular bone parameters

% decrease *	r	Adjusted r	Independent predictors		
BV/TV	0.46	0.41	-Tb.Th b, Conn.D b		
Tb.Th	0.66	0.66	-BS/BV c		
Tb.Sp	0.51	0.48	-Conn.D c, Tb.Th b		
Tb.N	0.66	0.64	-Tb.Th ^b , Conn.D ^b		
Conn.D	0.69	0.67	-Tb.Th ^b , Conn.D ^a , SMI ^a		
Tb.Stiffness 0.44		0.41	-Tb.Th ^c , -Tb.Sp ^b		

^{*:} Baseline parameters were correlated to percent decrease in all parameters for consistency. For the parameters that increased after OVX surgery (Tb.Sp), the percent decrease means a negative decrease.

Minus sign indicates negative correlation. a: p<0.05, b: p<0.01, c: p<0.001.

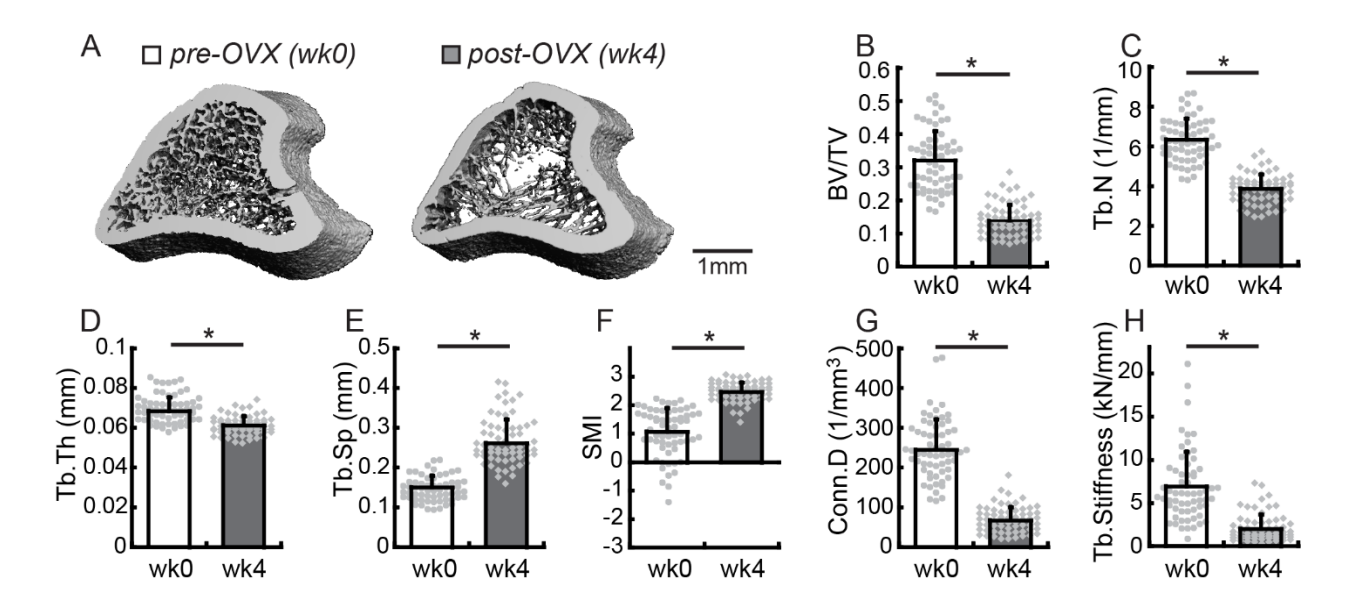


Figure 1. (A) Representative 3D renderings of the proximal tibia pre- (wk0) and post-OVX (wk4); (B-G) Trabecular structural parameters, including (B) BV/TV, (C) Tb.N, (D) Tb.Th, (E) Tb.Sp, (F) SMI, and (G) Conn.D at 0 and 4 weeks post-OVX. (H) FEA-derived Tb.Stiffness at 0 and 4 weeks post-OVX. * indicates significant changes over time (p<0.05).

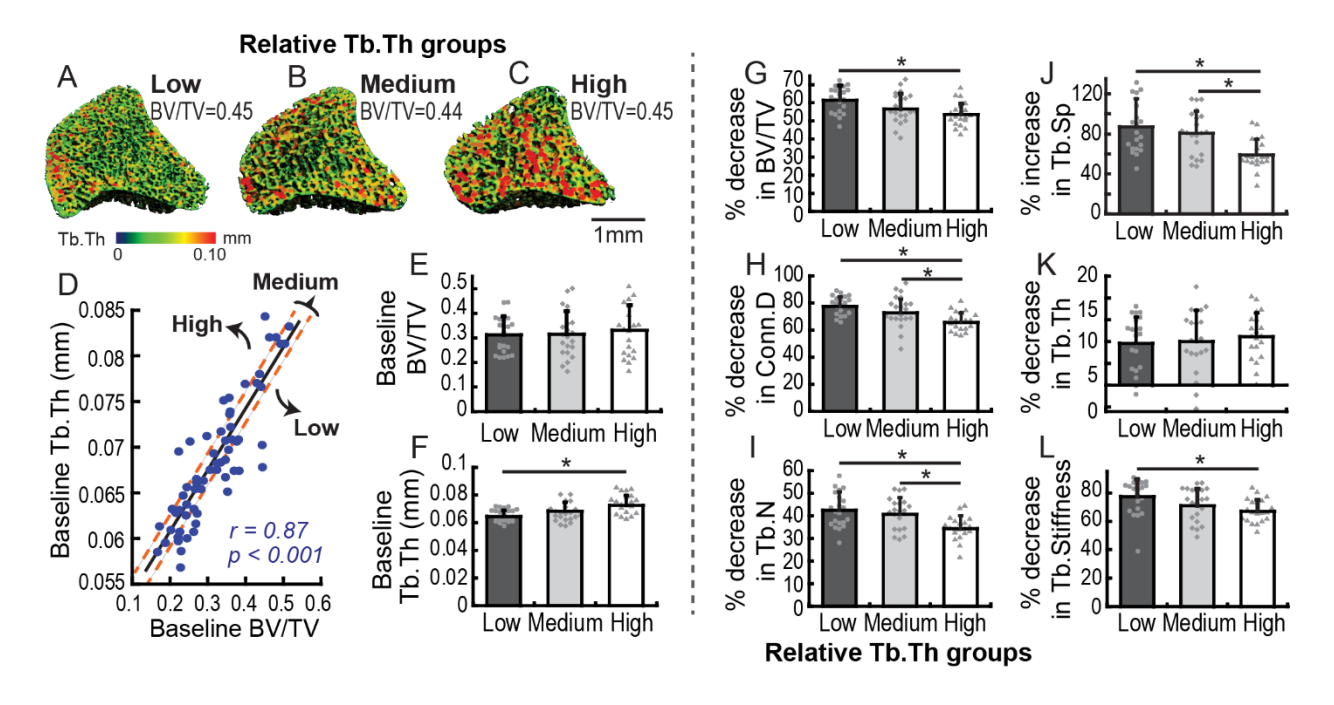


Figure 2. (A-C) Representative trabecular bone images in Low, Medium, and High relative Tb.Th groups. Heat maps correspond to local trabecular thickness values. (D) Rats were stratified into Low, Medium, and High relative Tb.Th by performing linear regression of baseline Tb.Th and BV/TV. (E) Baseline BV/TV was not different between Low, Medium, and High relative Tb.Th groups. (F) Comparisons of baseline Tb.Th among Low, Medium, and High relative Tb.Th groups. (G-L) % changes in trabecular bone parameters, including (G) BV/TV, (H) Conn.D, (I) Tb.N, (J) Tb.Sp, and (K) Tb.Th, in Low, Medium, and High relative Tb.Th groups over 4 weeks post-OVX. (L) % decrease in FEA-derived Tb.Stiffness in Low, Medium, and High relative Tb.Th groups. * indicates significant differences between groups (p<0.05).

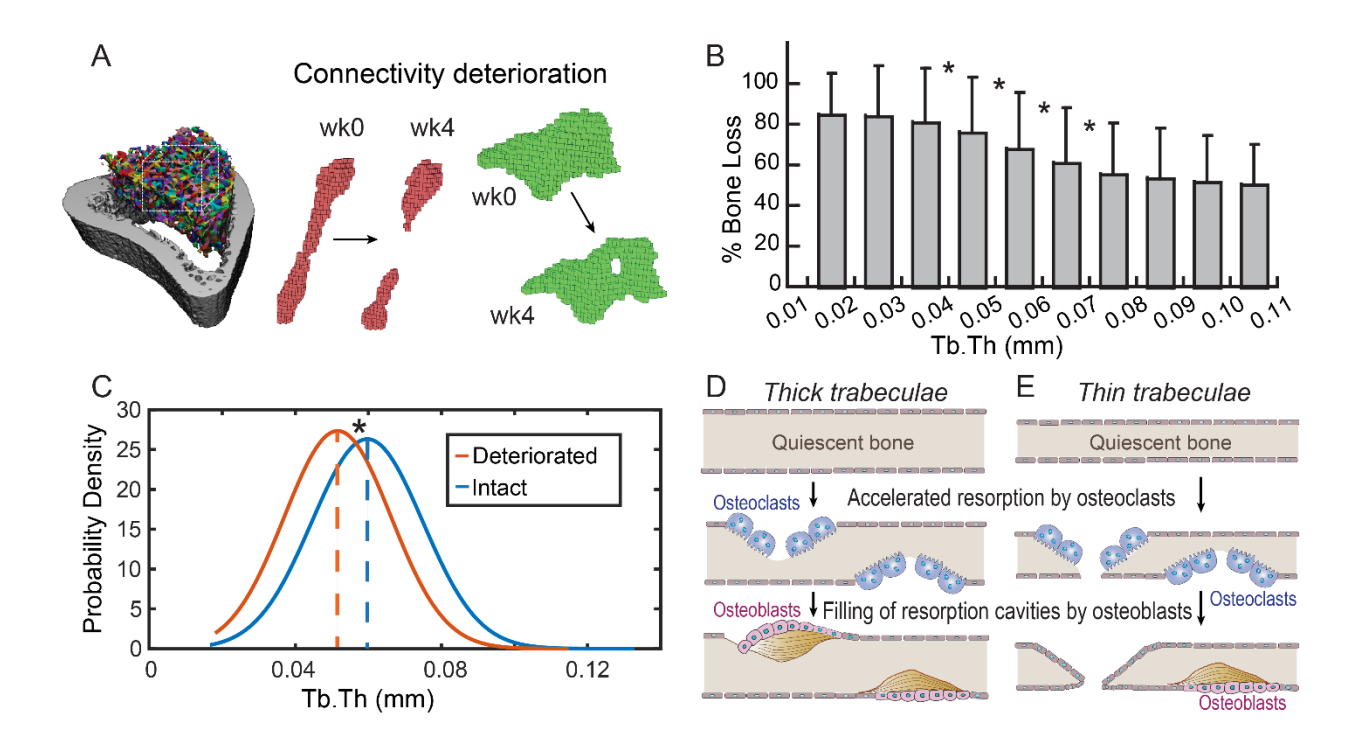


Figure 3. (A) Schematics of individual trabecular dynamics analysis. (B) % bone loss in individual trabeculae stratified by baseline thickness. (C) Probability density distribution of the baseline thickness of deteriorated and intact trabeculae. (D-E) Schematics of accelerated bone resorption followed by osteoblast repair in (D) a thick and (E) a thin trabecula. * indicates significant differences between groups (p<0.05).

Supplemental Data:

Table S1: Correlation coefficients (r) between baseline trabecular structural parameters

Baseline	BV/TV	Conn.D	SMI	Tb.N	Tb.Th	Tb.Sp	BS	BS/BV
Parameters	DV/1V	Conn.D	SIVII	10.11	10.111	10.5p	DS	DS/DV
BV/TV	1							
Conn.D	0.83 °	1						
SMI	-0.98 °	-0.78 °	1					
Tb.N	0.94 ^c	0.95 °	-0.90 c	1				
Tb.Th	0.88 °	0.51 °	-0.88 c	0.70 °	1			
Tb.Sp	-0.93 °	-0.91 °	0.87 °	-0.98 c	-0.69 c	1		
BS	0.53 °	0.62 °	-0.49 ^c	0.60 °	0.36 b	-0.57 °	1	
BS/BV	-0.95 °	-0.66 ^c	0.94 ^c	-0.81 °	-0.97 °	0.81 ^c	-0.43 °	1

^{*:} Minus sign indicates negative correlation. a: p<0.05, b: p<0.01, c: p<0.001.

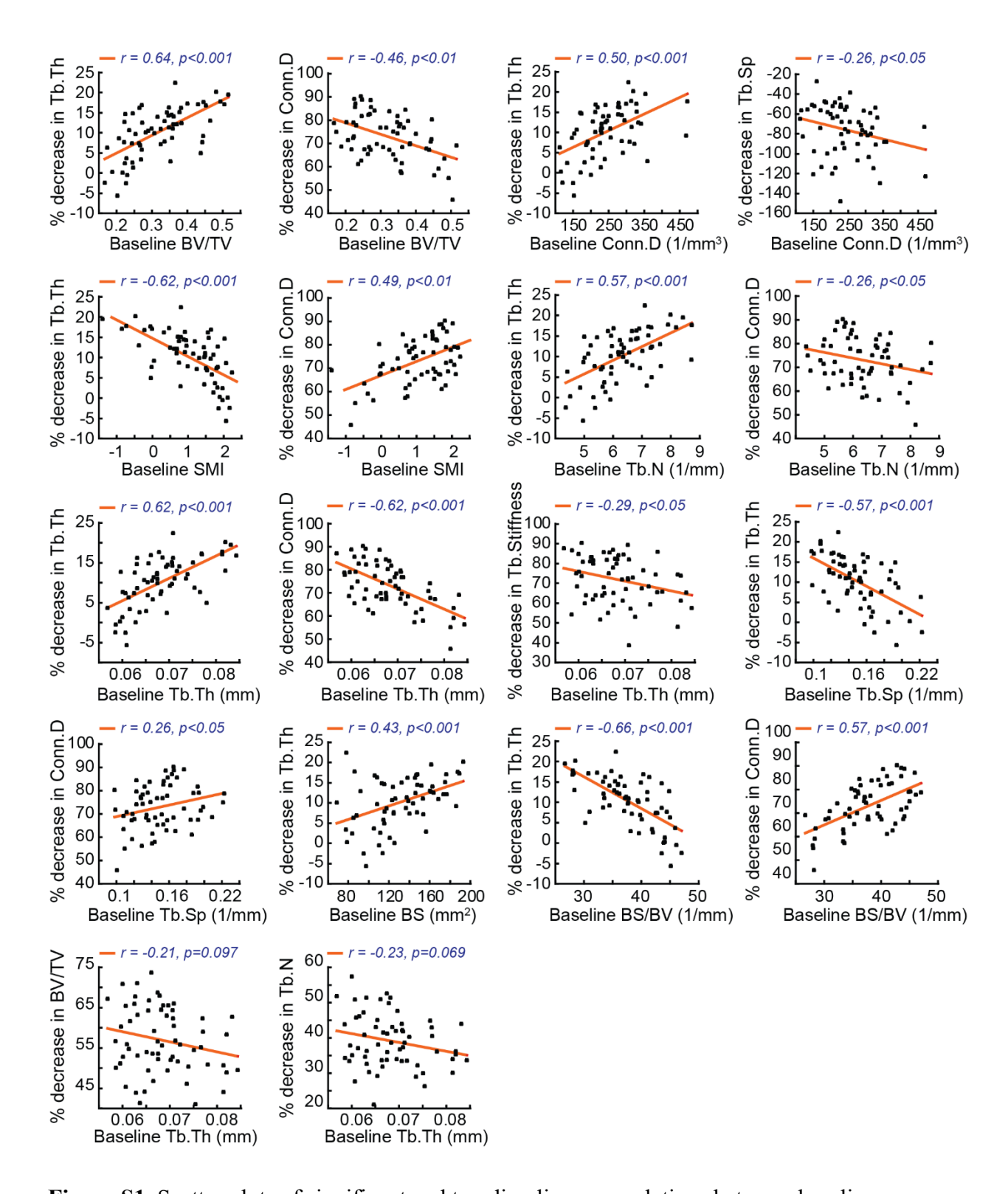


Figure S1. Scatter plots of significant and trending linear correlations between baseline trabecular parameters and % decrease in trabecular microstructural and mechanical properties.